Applied Mathematical Modelling 39 (2015) 682–692

Contents lists available at ScienceDirect

Applied Mathematical Modelling

journal homepage: www.elsevier.com/locate/apm

State-space estimation with a Bayesian filter in a coupled PDE system for transient gas flows

Ferdinand E. Uilhoorn *

Gas Engineering Division, Department of Environmental Engineering, Warsaw University of Technology, Nowowiejska 20, 00-653 Warsaw, Poland

ARTICLE INFO

Article history:
Received 16 July 2013
Received in revised form 21 May 2014
Accepted 30 June 2014
Available online 11 July 2014

Keywords:
Bayesian filtering
Monte Carlo methods
Particle filter
Unsteady compressible gas flow
Nonlinear/non-Gaussian
Two-step Lax–Wendroff

ABSTRACT

The accuracy of the first-principle models describing the evolution of gas dynamics in pipelines is sometimes limited by the lack of understanding of the gas transport phenomena. In this paper, a stochastic filtering approach is proposed based on a sequential Monte Carlo method to provide real-time estimates of the state in gas pipelines. After constructing a state-space model of the compressible single-phase flow based on the laws of conservation of mass and momentum, the optimal sequential importance resampling filter (SIR) is implemented. The state variables are updated with simulated measurements. The two-step Lax–Wendroff method is used for the discretization of the partial differential equations describing the gas model in both space and time to obtain finite-dimensional discrete-time state-space representations. The system states are then combined into an augmented state vector. The resulting nonlinear state-space model is used for the design of the particle filter that provides real-time estimations of the system states. Simulation results for a coupled PDE system describing an unsteady isothermal gas flow demonstrate the effectiveness of the proposed method. A sensitivity analysis is conducted to examine the performance of the filter for different model and observation error covariances and observation intervals.

1. Introduction

Mathematical modeling of compressible unsteady natural gas flows is important in the design of compressors and heat exchangers, orifice plates and sonic nozzle metering, conversion of gas volumes to the reference state, estimation of the line-pack [1], hydrate prevention [2,3] and leak detection [4,5]. Issa and Spalding [6], Deen and Reintsema [7] and Thorley and Tiley [8] developed the basic equations for a one-dimensional, unsteady, compressible single-phase flow, including the effects of wall friction and heat transfer. These models aim to predict accurately, the measurable quantities of pressure, temperature and mass flow in the pipeline. The uncertainties related to the model parameters, initial and boundary conditions cause model errors that can propagate in time. The model noise represents for example, diameter or roughness changes, fluctuations in gas composition, unknown ambient temperature changes, changes in soil moisture properties for buried pipelines, liquid dropout in a wet gas and so on. As a result, the final predictions can significantly differ from the reality. For this reason, a suitable approach of simulating gas dynamics in pipelines is to consider them as realizations of a stochastic process and find the most probable one or even the full probability distribution of the state. The availability of SCADA (Supervisory Control and Data Acquisition) measurements provides important but noisy information of the true system state.

* Tel.: +48 226213609; fax: +48 22 825 29 92.
E-mail address: frits.uilhoorn@is.pw.edu.pl

http://dx.doi.org/10.1016/j.apm.2014.06.021
0307-904X/

Nomenclature

Roman symbols

A	cross-sectional area
a_s	wave speed
$\mathbf{C}$	vector with source terms
c_p	specific heat at constant pressure
d	pipe diameter
e	measurement noise vector
$\mathbf{F}$	flux vector
$f(\cdot)$	generic nonlinear function
F_f	frictional force per unit length and time
g	gravitational acceleration
$h(\cdot)$	generic nonlinear function
L	pipeline length
$\dot{m}$	mass flow rate
N_{cell}	number of measurement nodes
N_k	number of measurement time steps
N_p	ensemble size
$\hat{N}_{eff}$	number of effective particles
p	probability density (mass) function
P	pressure
q	rate of heat transfer per unit length and unit time
Q	process noise covariance matrix
R	measurement noise covariance matrix
R_s	s constant
t	time
T	temperature
t_f	total simulation time
t_{obs}	observation time
u	system input vector
v	velocity
w	process noise vector
$\mathbf{W}$	vector of independent variables
x	spatial coordinate, state vector
$\hat{x}$	filtered estimate
y	measurement vector
z	compressibility factor

Greek symbols

δ	Dirac delta function
θ	inclination angle of pipe
λ	friction factor
ρ	density
$\mathbf{\Omega}$	spatial–temporal domain
ω	importance weight

Within in this framework, Bayesian filters [9,10] try to combine simulation and measurements to improve the accuracy and quantify uncertainties.

In case the stochastic, dynamical system is linear with additive Gaussian noises, the optimal solution of the estimator is found by minimizing the mean square error [11]. In this situation, the Kalman filter [12] provides the optimal solution of the filtering problem. Vianna et al. [13] applied the Kalman filter for the estimation of the temperature field in a deep sea pipeline carrying a homogeneous, isotropic fluid with constant thermal properties. The authors used simulated measurement data to estimate accurately the temperature of an oil–gas–water three-phase mixture in the pipeline with the aim to formulate preventive actions regarding hydrate formation. Ozawa and Sanada [14] and Sanada [15] used the Kalman filter to estimate the incompressible unsteady flow in an oil-hydraulic circuit. The Kalman filter is an effective tool for estimation but it is limited to linear models with additive Gaussian noises. Most real world systems are nonlinear, therefore several modifications of the Kalman filter have been developed, e.g., extended Kalman filter (EKF) [16] and the unscented Kalman

filter [11,17,18]. When the state functions are highly non-linear and the posterior density is non-Gaussian, the use of conventional filters, such as the EKF, may not provide satisfactory results [19].

One of the most successful approximation techniques in the Bayesian filtering domain is the sequential Monte Carlo (SMC) or particle filtering (PF). These techniques are a kind of recursive Bayesian filter based on particle representations of probability densities and can be applied to any state-space model. They generalize the traditional Kalman filtering methods and are not restricted by the assumption of linearity or Gaussian noise. SMC techniques approximate the probability density function (pdf) of the state variables by a set of random samples or particles with associated weights in order to determine the estimates based on these samples and weights. The particle set is updated and propagated by a process called sequential importance sampling (SIS). However, a common problem with the recursive algorithm such as the particle filter is the particle degeneracy where after several iterations the whole probability mass is focused on a few particles, whereas all the remaining particles have negligible weights. Gorden et al. [20] solved this problem by adding an extra step called resampling. This frequently used particle-filtering algorithm is known as sampling importance resampling (SIR).

In this paper, the PF-SIR filter is applied to a coupled PDE system describing a one-dimensional, unsteady, compressible gas flow. The objective is to estimate the gas pressure in a pipeline under transient conditions. The gas flow model is solved by the two-step Lax–Wendroff method [21]. A sensitivity analysis is conducted to examine the performance of the PF-SIR filter by using different observation and model error covariances and measurement intervals.

2. Materials and methods

2.1. Unsteady flow model in pipelines

A single-phase flow is described by coupled first-order hyperbolic partial differential equations derived from the conservation laws of mass, energy and momentum. These equations can be written as follows [8]:

$$\frac{\partial P}{\partial t}+v\frac{\partial P}{\partial x}+\rho a_s^2\frac{\partial v}{\partial x}=\frac{a_s^2}{c_pT}\left(1+\frac{T}{z}\left(\frac{\partial z}{\partial T}\right)_p\right)\left(\frac{q+F_fv}{A}\right), \tag{1}$$

$$\frac{\partial v}{\partial t}+v\frac{\partial v}{\partial x}+\frac{1}{\rho}\frac{\partial P}{\partial x}=-\frac{F_f}{A\rho}-g\sin(\theta), \tag{2}$$

$$\frac{\partial T}{\partial t}+v\frac{\partial T}{\partial x}+\frac{a_s^2}{c_p}\left(1+\frac{T}{z}\left(\frac{\partial z}{\partial T}\right)_p\right)\frac{\partial v}{\partial x}=\frac{a_s^2}{c_pP}\left(1-\frac{P}{z}\left(\frac{\partial z}{\partial P}\right)_T\right)\left(\frac{q+F_fv}{A}\right). \tag{3}$$

The convective acceleration terms, $v[\partial v/\partial x]$; $v[\partial P/\partial x]$ and the slope term are very small compared to the other terms and therefore can be neglected [22]. Kiuchi [23] ignored the convective terms due to the assumption of low flow velocity compared to the wave speed and states that this assumption is reasonable to most of the operation conditions in natural gas pipelines, while referring to the work of Guy [24] and Osiadacz [25]. However, Abbaspour and Chapman [26] showed that during rapid transients with increasing mass flow rate, the gas velocity increases and therefore, the convective inertia becomes more significant.

When analyzing the thermodynamics of gas flows, two extreme cases can be considered, namely isothermal flow and adiabatic flow. Isothermal flow is associated with slow transients and assumes that the gas has sufficient time to reach thermal equilibrium with its surroundings. It suggests an infinite heat capacity of the surroundings with constant temperature. Adiabatic flow is associated with fast dynamic changes without heat transfer between the gas and pipeline surroundings. Fast dynamic changes in the gas are important in situations of large fluctuations in demand or sudden rapid transients due to equipment failure or rapid closure of shut-off valves. In this situation, the slow effects of heat conduction between the gas pipeline and surroundings can be ignored. When friction effects are negligible, the flow can be considered as isentropic. In reality, heat transfer takes place and as a result there is no thermal equilibrium between the gas and its surroundings. In this situation, the conservation of energy must be included in the analysis. This results in a non-isothermal pipeline model, Eqs. (1)–(3) that includes the heat transfer term q accounting for the amount of heat exchange between the gas and its surroundings. The temperature change of the gas is a result of convective and conductive heat transfer, heat accumulation and Joule–Thomson effect. In case of buried pipelines, the difficulty is to define the soil temperature and properties such as heat capacity, thermal conductivity and diffusivity because they change over time as it alternately wets and dries. These quantities, which also differ along the pipeline, are difficult to predict. The Joule–Thomson effect is the temperature variation in the pipeline due to isenthalpic expansion or compression of the gas. Abbaspour and Chapman [26] showed that in case of rapid transient processes such as opening and closing a valve at the outlet, the gas should be treated in a non-isothermal manner because of the significant Joule–Thomson effect. Although, the non-isothermal model gives a more accurate description of the phenomenon, the increasing complexity and computation time can make it less useful for the optimal real-time control of gas pipelines. There should be a reasonable compromise between accuracy and computational complexity. Nevertheless, the simplification of the gas pipeline model together with uncertainties in model parameters and measurement inaccuracies of the boundary conditions induce errors and can propagate in time. Hence, to reduce the deviation in each time step between the computed values of the gas flow model and the actual system state, measurements are assimilated into the

model using the SIR particle filter. In this work, the gas model is simplified by assuming that the temperature changes within in the gas and heat exchange with its surroundings of the pipeline is negligible. The above assumptions lead to the following one-dimensional, isothermal formulation of the conservation equations:

$$\frac{\partial P}{\partial t}+\frac{a_s^2}{A}\frac{\partial \dot{m}}{\partial x}=0, \tag{4}$$

$$\frac{\partial \dot{m}}{\partial t}+A\frac{\partial P}{\partial x}+\frac{\lambda a_s^2}{2dA}\frac{\dot{m}|\dot{m}|}{P}=0, \tag{5}$$

where the pressure P and mass flow rate $\dot{m}$ are function of time t and distance x. The wave speed a_s is calculated from $\sqrt{zR_sT}$, where R_s is the specific gas constant and z the compressibility factor. Eqs. (4) and (5) can be written in the conservative form:

$$\frac{\partial \mathbf{W}}{\partial t}+\frac{\partial \mathbf{F}}{\partial x}+\mathbf{C}=0, \tag{6}$$

where

$$\begin{aligned}\mathbf{W}(x,t)&=\mathbf{W}=\begin{bmatrix}P\\ \dot{m}\end{bmatrix}\\ \mathbf{F}(\mathbf{W})&=\begin{bmatrix}\frac{a_s^2}{A}\dot{m}\\ AP\end{bmatrix}\\ \mathbf{C}(\mathbf{W})&=\begin{bmatrix}0\\ \frac{\lambda a_s^2}{2dA}\frac{\dot{m}|\dot{m}|}{P}\end{bmatrix}.\end{aligned} \tag{7}$$

The vectors **W**, **F**, and **C** represent the independent variables, their fluxes and source terms, respectively. The set of equations is one-dimensional, first order, nonlinear and hyperbolic. The initial conditions for the partial differential equations are obtained by setting the rates of change with time in Eqs. (4) and (5) equal to zero, i.e., $\partial P/\partial t=0$ and $\partial \dot{m}/\partial t=0$. The resulting equations for a horizontal pipe are

$$\frac{\partial \dot{m}}{\partial x}=0, \tag{8}$$

$$\frac{\partial P}{\partial x}=-\frac{\lambda a_s^2}{2dA^2}\frac{|\dot{m}|\dot{m}}{P}. \tag{9}$$

2.2. Two-step differential method Lax–Wendroff

To incorporate the particle filter, the state-space form is used to represent a mathematical model that simulates the dynamic process of gas transport in pipelines. Thorley and Tiley [8] gave an overview of different numerical techniques such as the method of characteristics, Lax–Wendroff method, implicit finite difference method and finite element method that solve the conservation equations for mass, momentum, and energy. In general a first order-order approximation is not sufficient accurate for modeling unsteady gas flow in pipelines. Therefore, the attention is focused on second-order methods. Kiuchi [23], Poloni et al. [27] and Greyvenstein [28] used the two-step Lax–Wendroff method together with the method of characteristics and implicit methods for the simulation of transient flows in pipelines. In this work, the two-step Lax–Wendroff method is applied. The advantage of this explicit finite-difference method is that the discretized equations can be easily formulated as a state-space model. The two-step Lax–Wendroff scheme for Eq. (6) is as follows:

In the first step:

$$\mathbf{W}_{i+1/2}^{j+1/2}=\frac{1}{2}(\mathbf{W}_{i+1}^{j}+\mathbf{W}_{i}^{j})-\frac{\Delta t}{2\Delta x}(\mathbf{F}_{i+1}^{j}-\mathbf{F}_{i}^{j})-\frac{\Delta t}{4}(\mathbf{C}_{i+1}^{j}+\mathbf{C}_{i}^{j}), \tag{10}$$

and in the second step:

$$\mathbf{W}_{i}^{j+1}=\mathbf{W}_{i}^{j}-\frac{\Delta t}{\Delta x}\left(\mathbf{F}_{i+1/2}^{j+1/2}-\mathbf{F}_{i-1/2}^{j+1/2}\right)-\frac{\Delta t}{2}\left(\mathbf{C}_{i+1/2}^{j+1/2}+\mathbf{C}_{i-1/2}^{j+1/2}\right). \tag{11}$$

However, an obvious disadvantage of this scheme is that the time-steps are restricted by the Courant–Friederich–Lewy (CFL) condition [29]. This scheme is stable if the CFL condition holds

$$\left|\left(\max_k a_{s,k}\right)\frac{\Delta t}{\Delta x}\right|\leq 1, \tag{12}$$

where the parameter $a_{s,k}$ represents the largest wave speed in the entire solution domain at time level k.

2.3. Bayesian estimation of the state-space model

To study and make an inference about the gas dynamics in pipelines at least two models are needed. The first one describes the evolution of the state in time and the second one relates the noisy measurements to the state. As a result of uncertainties in modeling, as well as inaccuracies in measurements, noise terms in Eq. (13) are added to obtain a stochastic equation. Therefore, the dynamic system is represented by a stochastic process $x_k \in \mathbb{R}^n$, whose temporal is given by the state equation:

$$x_{k+1} = f(x_k, u_k) + w_k, \tag{13}$$

where $u_k \in \mathbb{R}^p$ stands for the input. In order to estimate the state vector x_k at discrete times, system observations are used, which are realization of the stochastic process $y_k \in \mathbb{R}^m$ governed by the measurement equation:

$$y_{k+1} = h(x_{k+1}) + e_{k+1}. \tag{14}$$

Note that the functions $f : \mathbb{R}^p \times \mathbb{R}^n \to \mathbb{R}^m$ and $h : \mathbb{R}^n \to \mathbb{R}^m$ are assumed nonlinear. The subscript $k = 1, 2, 3\ldots$, denotes a time instant t_k. The process noise $w_k \in \mathbb{R}^n$ and measurement noise $e_k \in \mathbb{R}^m$ are assumed to be white zero-mean Gaussian random sequences, i.e., $w_k \sim \mathcal{N}(0, Q_k)$ and $e_k \sim \mathcal{N}(0, R_k)$, which fulfil the following properties:

$$\mathbb{E}[w_{k1} \cdot e_{k2}] = 0 \quad \forall k_1, k_2, \tag{15}$$

$$\mathbb{E}[e_{k1} \cdot e_{k2}] = 0 \quad \mathbb{E}[w_{k1} \cdot w_{k2}] = 0 \quad \forall k_1 \neq k_2, \tag{16}$$

$$\mathbb{E}[w_k \cdot w_k] = Q_k \quad \mathbb{E}[e_k \cdot e_k] = R_k, \tag{17}$$

where Q_k and R_k are covariance matrices.

In the Bayesian framework, the idea is to calculate recursively the pdf $p(x_k|y_{1:k})$, where x_k is the state vector at time k and $y_{1:k}$ is the set of measurements up to time step k. It is assumed that the initial pdf $p(x_0|y_0) \equiv p(x_0)$ is given and the pdf $p(x_k|y_{1:k})$ is obtained recursively by a prediction step and update step. In the prediction step, the estimate of the pdf of the most recent state of the system $p(x_{k-1}|y_{1:k-1})$ is propagated by the state-space model one-step ahead. It calculates $p(x_k|y_{1:k-1})$ from $p(x_{k-1}|y_{1:k-1})$ using the Chapman–Kolmogorov equation [30]

$$p(x_k|y_{1:k-1}) = \int p(x_k|x_{k-1})p(x_{k-1}|y_{1:k-1})dx_{k-1}. \tag{18}$$

In the update step, the predicted density is compared with the measurement y_k and consequently transformed in line with Bayes' rule [20]

$$p(x_k|y_{1:k}) = \frac{p(y_k|x_k)p(x_k|y_{1:k-1})}{p(y_k|y_{1:k-1})}, \tag{19}$$

where $p(y_k|y_{1:k-1})$ is the normalizing factor of the state x_k, i.e.,

$$p(y_k|y_{1:k-1}) = \int p(y_k|x_k)p(x_k|y_{1:k-1})dx_k. \tag{20}$$

The two latter equations represent the optimal Bayesian solution of the nonlinear state estimation problem. In practice, the posterior probability $p(x_k|y_{1:k})$ cannot be solved analytically. Hence, approximate filters are used to find suboptimal solutions.

2.4. Optimal sequential importance resampling filter

The particle filter is a sequential Monte Carlo method, which approximates the above equations for a general nonlinear system with arbitrarily process and measurement noises. The posterior pdf $p(x_{0:k}|y_{1:k})$ is characterized by the set of N pairs $\{x^i_{0:k}, \omega^i_k\}_{i=1}^N$ of particles, where $\{x^i_{0:k}, i = 0, \ldots, N\}$ with their associated weights $\{\omega^i_k, i = 1, \ldots, N\}$ and $x_{0:k} = \{x_j, j = 0, \ldots, k\}$. These pairs approximate the true pdf by the formula:

$$p(x_{0:k}|y_{1:k}) \approx \sum_{i=1}^{N} \omega^i_k \delta(x_{0:k} - x^i_{0:k}), \tag{21}$$

where δ is the Dirac delta function. The weights are normalized such that $\sum_{i=1}^N \omega^k_i = 1$ and selected according to the principle of importance sampling [31]. A common problem with the recursive algorithm is the particle degeneracy. This means that after a few iterations the probability mass is focused on a few particles while the remaining particles have a negligible weight. Degeneracy is typically measured by an estimate of the effective sample size [30]:

$$\hat{N}_{eff} = \left(\sum_{i=1}^{N} (\omega^i_k)^2 \right)^{-1}. \tag{22}$$

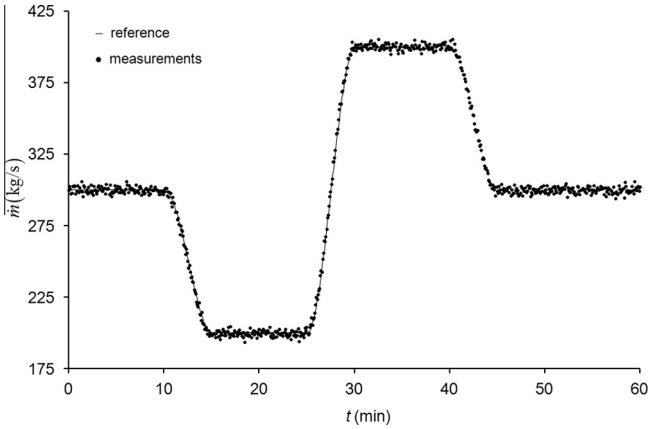

Fig. 1. Simulated mass flow measurements at the boundary, $\dot{m}(L,t)$.

A smaller $\hat{N}_{eff}$ means a larger variance for the weights, hence more degeneracy. To resolve this problem a resampling procedure is used. There are many variations of particle filters, which employ various importance densities and resampling algorithms [30]. The pseudo-code description of the particle filter and resampling are provided in the appendix.

3. Results and discussion

A series of numerical simulations were conducted for a high-pressure pipeline transporting natural gas. The computations were done in the programming and calculation environment MATLAB™. The pipeline has a length of 177 km and a diameter of 1.4 m. The friction factor λ is 0.015 and assumed constant throughout the pipeline. The density of the natural gas at standard conditions ρ_n is 0.784 kg/m^3, the specific gas constant R_s is 474.5 J kg^{-1} K^{-1} and the compressibility factor z is 0.9. The isothermal temperature is 300 K. The true state was identified by the numerical solution of Eqs. (4) and (5) using the two-step Lax–Wendroff scheme. The simulation is started with the initial conditions defined by Eqs. (8) and (9). The spatial–temporal domain is given by $\Omega = \{(x,t)\colon 0 \leqslant x \leqslant L,\ 0 \leqslant t \leqslant t_f\}$, whereas the total simulation time t_f is 3600 with a time step $\Delta t = 5$ s and spatial step $\Delta x = 4425$ m. The CPU efficiency of the explicit method is constrained by the CFL condition, which restricts large time steps. For the observation model, simulated pressure measurements were used by adding a random Gaussian error, which reflects the randomized nature of the real field data. An observation error with a distribution $\mathcal{N}(0, 10^{-4})$ in MPa^2 is added to the true state. The observation interval Δt_{obs} is 5 s and the measurements are obtained in 10 evenly distributed nodes along the 177 km pipeline. Figs. 1 and 2 illustrate the observations at the boundary conditions $P(0,t)$ and $\dot{m}(L,t)$, which were computed by adding to the reference situation a random noise with a Gaussian distribution $\mathcal{N}(0, 10^{-4})$ and $\mathcal{N}(0,4)$ in MPa^2 and (kg/s)^2, respectively.[1] The model error variance is set 10% smaller than the observation error variance, i.e., 9×10^{-5} MPa^2 and 3.6 (kg/s)^2. It represents the randomness and uncertainly in the simulation of transient flow in gas pipelines. Figs. 1 and 2, depict the simulated mass flow rate and pressure measurements at the boundaries, respectively. Fig. 3 shows, the spatial–temporal evolution obtained from the numerical simulation. The evolutionary trajectories corresponding to the values at the finite-difference node points used for the PF-SIR filter are marked with dark solid lines on the 3-D surface. Simulations showed that the gas velocity in the spatial–temporal domain remained between 2.1 and 4.3 m/s, while the calculated wave speed is 357.9 m/s. This supports the earlier assumption, that the convective acceleration terms in the gas flow model can be neglected.

The state tracking values at the end and midpoint of the pipeline are presented in Figs. 4 and 5. The ensemble size was set to 100 and to reduce the influence of the random error, 100 independent simulations with different random generator seeds were conducted.

The effectiveness of the SIR particle filter was demonstrated by calculating the space- and time averaged root-mean-square error (RMSE) between the results from the finite-difference scheme and the SIR particle model. The space- and time averaged RMSE for one Monte Carlo run is defined by:

$$\text{RMSE} = \frac{1}{N_{cells}} \sum_{i=1}^{N_{cell}} \sqrt{\frac{1}{N_k} \sum_{k=1}^{N_k} (x_k^i - \hat{x}_k^i)^2}, \tag{23}$$

where x_k^i and $\hat{x}_k^i$ are the true and filtered estimated pressure values at cell i and time step k, N_{cell} is the number of measurement nodes and N_k is the number of measurement time steps. Fig. 6 shows the RMSE performance for different ensemble

[1] MATLAB™ *randn*-function is used to generate quasi-random numbers.

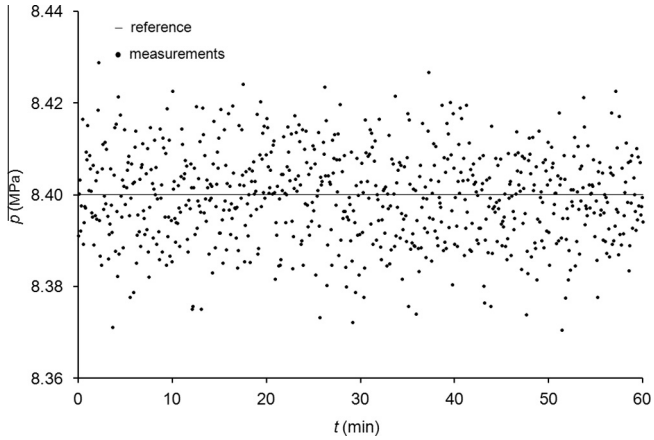

Fig. 2. Simulated pressure measurements at the boundary, $P(0,t)$.

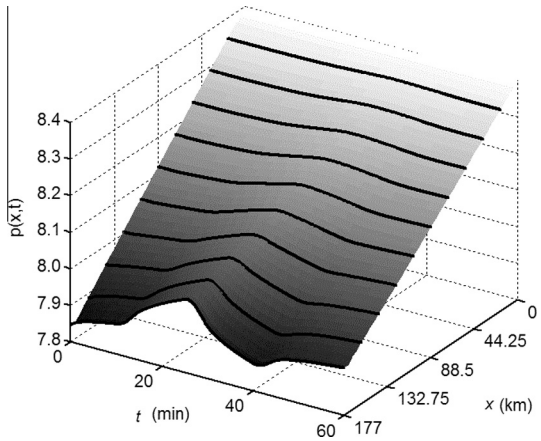

Fig. 3. Spatial–temporal evolution of the PDE system (4) and (5).

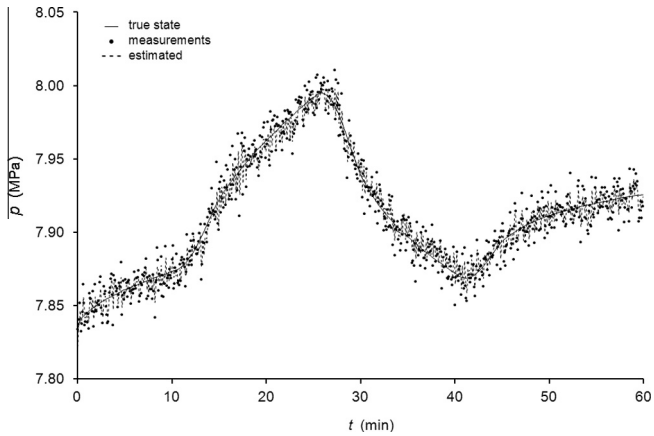

Fig. 4. True, measured and estimates of the PF-SIR at the end of the pipeline.

sizes $N_p \in \{10, 50, 100, 150\}$ and simulation runs. The difference in RMSE between a particle size of 100 and 150 is relatively small.

In this section, the filter stability and error sensitivities are evaluated for different model and observation error covariances. First, the model error variance is set 10% and 50% less and greater than the observation noise variance of

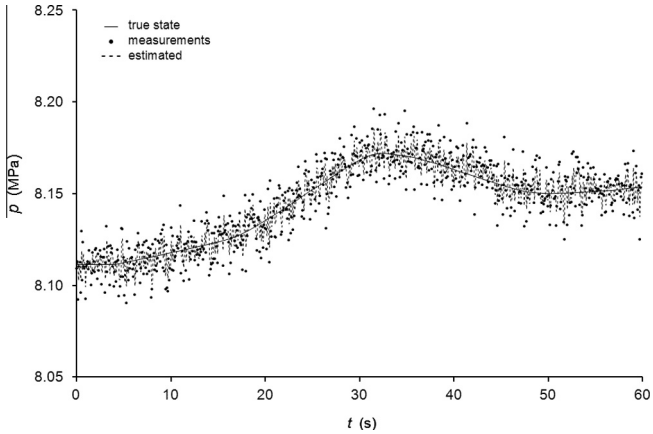

Fig. 5. True, measured and estimates of the PF-SIR at the mid-point of the pipeline.

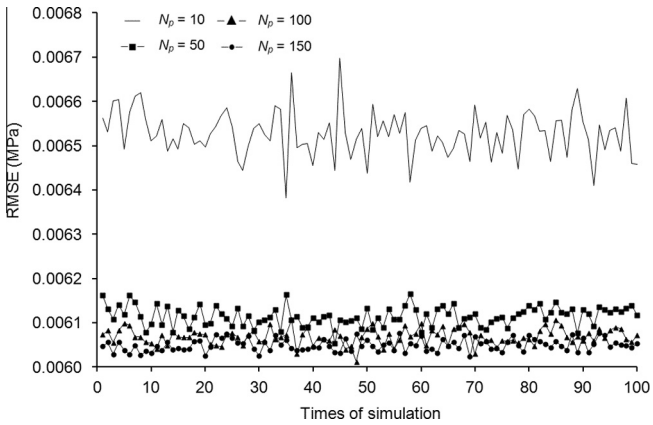

Fig. 6. RMSE as function of simulation runs.

10^{-4} MPa^2 and 4 (kg/s)^2. The results are presented in Fig. 7 and it can be inferred that a lower model error variance improves the RMSE. When the model noise is significant smaller than the measurements noise, the particle filter has difficulties to track the changes in the boundary conditions fast enough. The small lag between the true and estimated value is illustrated in Fig. 8. In this situation, the model error variance is set 90% below the observation error. In case, the model error is greater than the observation error, the RMSE values becomes worse.

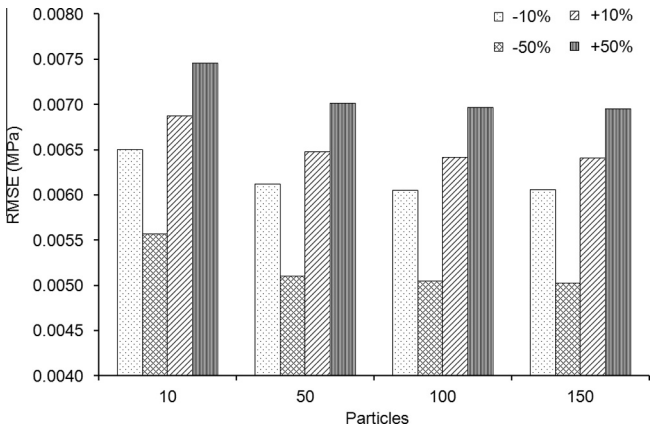

Fig. 7. RMSE for different model error variances and particle numbers, 100 independent runs and $\Delta t_{obs} = 5$.

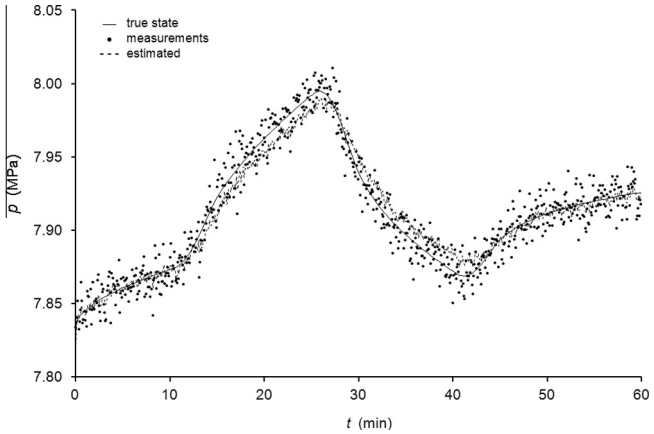

Fig. 8. True, measured and estimates of the PF-SIR at the end of the pipeline with model noise variance 90% less than the measurement noise variance for both pressure and mass flow rate.

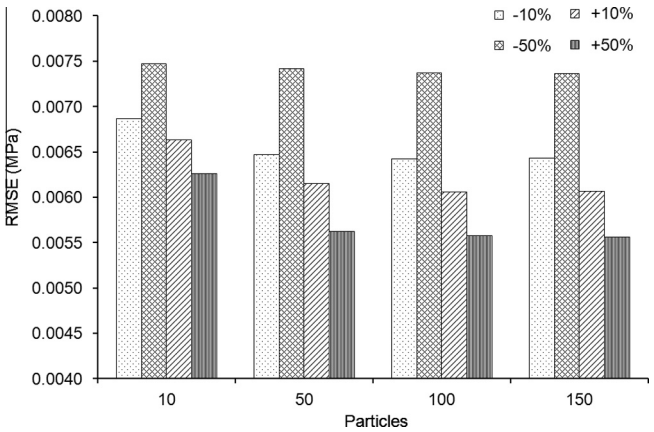

Fig. 9. RMSE for different observation error variances and particle numbers, 100 independent runs and $\Delta t_{obs} = 5$.

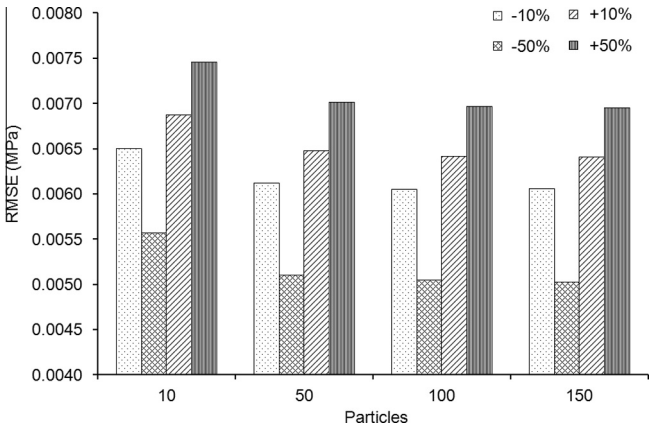

Fig. 10. RMSE for different model error variances and particle numbers, 100 independent runs and $\Delta t_{obs} = 10$.

In the next step, the observation error variances are set 10% and 50% less and greater than the model error variance values of 10^{-4} MPa^2 and 4 (kg/s)^2. The results are presented in Fig. 9 and show that the RMSE becomes worse when the distance in variance between model and observation error increases. The opposite is true when the model error variance is greater than the observation error variance. In the last part, the filter performance with respect to the measurement rate is examined. When the observation interval is changed to 1 observation every 10 s, the results improve. This is illustrated in Figs. 10 and 11.

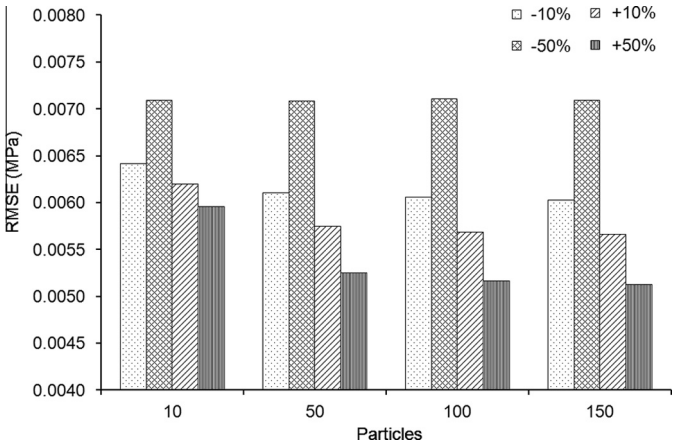

Fig. 11. RMSE for different observation error variances and particle numbers, 100 independent runs and $\Delta t_{obs} = 10$.

4. Conclusion

Within the Bayesian framework, the system model containing weak knowledge about the initial state, can achieve more accurate information about the state via assimilation of measurement data. In the unsteady gas flow model, the particle filter reduces the deviation in each time step by combining the observation data with the model values. The degeneracy problem of the SIS particle filter has been overcome by using sequential importance resampling. The performance of the filter was investigated by computing the space- and time averaged RMSE for different covariances of the model and observation random error. An ensemble size of 100 showed a good compromise between accuracy and computation time. When the model noise is significant smaller than the measurement noise, the filter has difficulties to track the changes. In case the observation variance is fixed, a lower model error variance improves the results and increasing the variance the RMSE becomes worse. The opposite is observed when the model error is fixed and the observation error variance is varied. By extending the observation interval, the RMSE is decreasing.

Appendix A. Pseudo-code description of the particle filter and resampling

Algorithm 1: SIR particle filter

$\left[\{x_k^i, \omega_k^i\}_{i=1}^N\right] = \mathrm{SIR}\left[\{x_{k-1}^i, \omega_{k-1}^i\}_{i=1}^N, y_k\right]$

Initialize : $k = 0, x_0^i \sim p(x_0),\ i = 1, 2, \ldots, N$ Let $k = 1$

FOR $i = 1 : N$

Draw $x_k^i \sim q(x_k^i | x_{k-1}^i, y_k)$

Assign particle a weights, ω_k^i, according to

$$\omega_k^i \propto \omega_{k-1}^i \frac{p(y_k|x_k^i)p(x_k^i|x_{k-1}^i)}{q(x_k^i|x_{k-1}^i, y_k)}$$

END FOR

Calculate total weight : $t = \sum_{j=1}^N \omega_k^i$

FOR $i = 1 : N$

Normalize : $\omega_k^i = t^{-1}\omega_k^i$

END FOR

$\left[\left\{x_k^{j*}, \omega_k^j, -\right\}_{j=1}^N\right] = \mathrm{Resample}\left[\{x_k^i, \omega_k^i\}_{i=1}^N\right]$

Algorithm 2: Resampling

$\left[\left\{x_k^{j^*}, \omega_k^j, i^j\right\}_{j=1}^N\right] = \text{Resample}[\{x_k^i, \omega_k^i\}_{i=1}^N]$
Initialize the cumulative sum of weights(CSW) : $c_1 = \omega_k^1$
FOR $i = 2 : N$
  Compute CSW : $c_i = c_{i-1} + \omega_k^j$
END FOR
Start at the bottom of the CSW : $i = 1$
Draw starting point : $u_1 \sim \mathcal{U}(0, N^{-1})$
FOR $j = 1 : N$
  Move along the CSW : $u_j = u_1 - N^{-1}(j-1)$
  WHILE $u_j > c_i$
    $i = i + 1$
  END WHILE
    Assign sample : $x_k^{j^*} = x_k^j$
    Assign weight : $\omega_k^j = N^{-1}$
    Assign parent : $i^j = i$
END FOR

References

[1] F.E. Uilhoorn, Dynamic behaviour of non-isothermal compressible natural gases mixed with hydrogen in pipelines, Int. J. Hydrogen Energy 34 (16) (2009) 6722–6729.
[2] A. Osiadacz, F.E. Uilhoorn, M. Chaczykowski, Computation of hydrate phase equilibria and its application to the Yamal–Europe gas pipeline, Pet. Sci. Technol. 27 (2) (2009) 208–225.
[3] F.E. Uilhoorn, Evaluating the risk of hydrate formation in CO_2 pipelines under transient operation, Int. J. Greenhouse Gas Control 14 (2013) 177–182.
[4] B. Brunone, M. Ferrante, Detecting leaks in pressurized pipes by means of transients, Automatica 39 (2001) 1–9.
[5] H.P. Reddy, S. Narasimhanb, S.M. Bhallamudia, S. Bairagic, Leak detection in gas pipeline networks using an efficient state estimator. Part-I: theory and simulations, Comput. Chem. Eng. 35 (4) (2011) 651–661.
[6] R.I. Issa, D.B. Spalding, Unsteady one-dimensional compressible frictional flow with heat transfer, J. Mech. Eng. Sci. 14 (6) (1972) 365–369.
[7] J.K. Deen, S.R. Reintsema, Modeling of high-pressure gas transmission lines, Appl. Math. Model. 7 (1983) 268–273.
[8] A.R.D. Thorley, C.H. Tiley, Unsteady and transient flow of compressible fluids in pipelines – a review of theoretical and some experimental studies, J. Heat Fluid Flow 8 (1) (1987) 3–15.
[9] J. Kaipio, E. Somersalo, Statistical and Computational Inverse Problems, Springer-Verlag, Berlin, 2004. pp. 1–339.
[10] P. Maybeck, Stochastic Models, Estimation and Control, Academic Press, New-York, 1979. pp. 1–444.
[11] B. Ristic, S. Arulampalam, N. Gordon, Beyond the Kalman Filter: Particle Filters for Tracking Application, Artech House Publishers, 2004. pp. 1–318.
[12] R.E. Kalman, A new approach to linear filtering and prediction problems, Trans. ASME – J. Basic Eng. 82 (Series D) (1960) 34–45.
[13] F.L.V. Vianna, H.R.B. Orland, G.S. Dulikravich, Estimation of the temperature field in pipelines by using the Kalman filter, in: 2nd International Congress of Serbian Society of Mechanics, Serbia, 2009.
[14] A. Ozawa, K.A. Sanada, Kalman filter for estimating transient pressure and flow rate in a pipe, in: SICE Annual Conference, Japan, 2011.
[15] K. Sanada, Using a Kalman filter to estimate unsteady flow, Int. J. Autom. Technol. 6 (4) (2012) 440–444.
[16] B.D.O. Anderson, J.B. Moore, Optimal Filtering, Prentice-Hall, Englewood Cliffs, 1979. pp. 1–367.
[17] S. Julier, J. Uhlmann, A general method for approximating nonlinear transformations of probability distributions. Robotics Research Group, Department of Engineering Science, University of Oxford, 1996.
[18] S. Julier, J. Uhlmann, Unscented filtering and nonlinear estimation, Proc. IEEE 92 (3) (2004) 401–422.
[19] T. Chen, J. Morris, E. Martin, Particle filters for the estimation of a state space model, Comput. Aided Chem. Eng. 18 (C) (2004) 613–618.
[20] N.J. Gordon, D.J. Salmond, A.F.M. Smith, Novel approach to nonlinear/non-Gaussian Bayesian state estimation, IEE Proc. F Radar Signal Process. 140 (2) (1993) 107–113.
[21] R.D. Richtmyer, K.W. Morton, Difference Methods for Initial Value Problems, Interscience Publishers, New-York, 1967.
[22] M.H. Chaudhry, Applied Hydraulic Transients, Van Nostrand Reinhold, New-York, 1987.
[23] T. Kiuchi, An implicit method for transient gas flows in pipe networks, Int. J. Heat Fluid Flow 15 (8) (1994) 378–383.
[24] J.J. Guy, Computation of unsteady gas flow in pipe networks, in: Symposium Series No. 23: Institute of Chemical Engineers, London, 1967.
[25] A. Osiadacz, Simulation of transient gas flows in networks, Int. J. Numer. Methods Fluids 4 (1) (1984) 13–24.
[26] M. Abbaspour, K.S. Chapman, Nonisothermal transient flow in natural gas pipeline, J. Appl. Mech. 75 (3) (2008) 031018-1–031018-8.
[27] M. Poloni, D.E. Winterbone, J.R. Nichols, Comparison of unsteady flow calculations in a pipe by the method of characteristics and the two-step differential Lax–Wendroff method, Int. J. Mech. Sci. 29 (5) (1987) 367–378.
[28] G.P. Greyvenstein, An implicit method for the analysis of transient flows in pipe networks, Int. J. Numer. Methods Eng. 53 (2002) 1127–1143.
[29] R. Courant, K.O. Friedrichs, H. Lewy, Über die partiellen Differenzengleichungen der mathematischen Physik, Math. Ann. 100 (1928) 32–74.
[30] S. Arulampalam, S. Maskell, N. Gordon, T. Clapp, A tutorial on particle filters for online nonlinear/non-Gaussian Bayesian tracking, IEEE Trans. Signal Process. 50 (2) (2002) 174–188.
[31] N. Bergman, Recursive Bayesian estimation: navigation and tracking applications,. Linkoping University, Sweden, 1999.